



CHORUS

This is the accepted manuscript made available via CHORUS. The article has been published as:

Pure negatively charged state of the NV center in n-type diamond

Yuki Doi, Takahiro Fukui, Hiromitsu Kato, Toshiharu Makino, Satoshi Yamasaki, Toshiyuki Tashima, Hiroki Morishita, Shinji Miwa, Fedor Jelezko, Yoshishige Suzuki, and Norikazu Mizuochi

Phys. Rev. B **93**, 081203 — Published 3 February 2016

DOI: [10.1103/PhysRevB.93.081203](https://doi.org/10.1103/PhysRevB.93.081203)

Pure negatively charged state of the NV center in n-type diamond

Yuki Doi¹, Takahiro Fukui¹, Hiromitsu Kato^{2,3}, Toshiharu Makino^{2,3}, Satoshi Yamasaki^{2,3},
Toshiyuki Tashima¹, Hiroki Morishita¹, Shinji Miwa¹, Fedor Jelezko⁴, Yoshishige Suzuki¹,
and Norikazu Mizuochi^{1,3,a)}

¹*Graduate School of Engineering Science, Osaka University, Toyonaka, Osaka 560-8531, Japan*

²*Energy Technology Research Institute, National Institute of Advanced Industrial Science and
Technology (AIST), Tsukuba, Ibaraki 305-8568, Japan*

³*CREST, Japan Science and Technology Agency, Kawaguchi, Saitama 332-0012, Japan*

⁴*Institut für Quantenoptik, Universität Ulm, Albert-Einstein-Allee 11, 89081 Ulm, Germany*

^{a)} Electronic mail: mizuochi@mp.es.osaka-u.ac.jp

Abstract

Optical illumination to negatively charged nitrogen-vacancy centers (NV^-) inevitably causes stochastic charge-state transitions between NV^- and neutral charge state of the NV center. It limits the steady-state-population of NV^- to 5% at minimum (~ 610 nm) and 80% (~ 532 nm) at maximum in intrinsic diamond depending on the wavelength. Here, we show Fermi level control by phosphorus doping generates $99.4 \pm 0.1\%$ NV^- under 1 μ W and 593 nm excitation which is close to maximum absorption of NV^- . The pure NV^- shows a five-fold increase of luminescence and a four-fold enhancement of an optically detected magnetic resonance under 593 nm excitation compared with those in intrinsic diamond.

1 Nitrogen-vacancy (NV) centers in diamond are the most promising candidate for various
2 applications such as quantum information science [1–8], magnetometry [9–13], and biosensing [14–
3 16]. For these applications, controlling the charge state of the NV centers is crucial, because optical
4 initialization and readout of the spin state of the NV centers are only possible in negatively charged
5 one (NV^-). However, upon illumination, the NV centers undergo stochastic charge-state transitions
6 between NV^- and neutral charge state of the NV center (NV^0) [17,18]. For example, upon excitation
7 around 580 nm, where NV^- has the highest absorption [17,19], NV^- easily turns into the NV^0 and the
8 steady-state-population of NV^- decreases to about 10%, which could be revealed from single-shot
9 charge-state measurements [17]. Therefore, illumination at 532 nm is usually used in the experiment
10 of NV^- . This charge-state interconversion occurs upon illumination at any wavelength, so the steady-
11 state NV^- population is always less than 75%–80% [17,20].

12 Generating a pure state including the charge state, close to 100% NV^- population, is very
13 important for quantum information applications. Studies involving the pre-selection and reset of the
14 charge state were carried out to achieve high-fidelity operation because of the instability of the
15 charge states [1,4,5]. However, this approach makes scaling up of diamond quantum registers more
16 challenging. Furthermore, single-shot readout of a nuclear spin indicates that the spin-flip probability
17 of the conditional gate operation decreases because of the stochastic charge-state transitions [6,21].
18 In addition, such charge-state transitions lead to spectral diffusion [18,22,23] of the zero-phonon line
19 of NV^- , which reduces the efficiency of two-photon quantum interference [4]. For nanoscale sensing
20 applications, it is crucial to keep NV^- stable near the surface for high spatial resolution [15];
21 however, NV^- near the surface is unstable [24]. In addition, high-contrast fluorescence switching
22 between pure bright NV^- and the pure dark state (NV^0) is also very important for super-resolution
23 microscopy [25].

24 Previously, NV charge states were controlled by heavy neutron irradiation [26], surface
25 termination [27–29], and combined optical and electrical operations [30–33]. Most of them were

1 investigated by photoluminescence (PL) spectra, which only reveals a ratio of the charge states of the
2 bright state. On the other hand, single-shot charge-state measurements can reveal the ratio of NV^-
3 and NV^0 during illumination. Recently, deterministic control from NV^- to NV^0 by a purely electrical
4 operation was revealed from the single-shot charge-state measurements [34]. Doping with nitrogen is
5 considered to be one way to control the NV^- population. Nitrogen donors (P1 centers) can donate
6 electrons to NV^0 in the dark region (without laser illumination), thereby changing its state to NV^- ,
7 because the activation energy ($E_A = 1.70$ eV) of P1 is less than the energy difference between the
8 acceptor level, labeled $(-/0)$, of the NV center [35] and the conduction-band edge, as shown in Fig.
9 1(a). Recently, charge states of ensemble NV centers were modulated by ion-implantation of
10 phosphorus and boron atoms [36]. However, pure NV^- charge state, which can be revealed by the
11 single-shot charge-state measurements, has not yet been realized in nitrogen doping and ion-
12 implantation of phosphorus. Based on the activation energy, phosphorus doping during chemical
13 vapor deposition (CVD) appears promising because that of phosphorus ($E_A = 0.57$ eV) [37] is much
14 less than that of P1. It should be noted that, so far, n-type conductivity in diamond has been only
15 realized by the CVD synthesis technique. In the present study, we quantitatively investigate the
16 charge-state population of NV centers by using single-shot readout measurements in slightly
17 phosphorus-doped n-type diamond. We obtain a pure NV^- population ($> 99\%$ NV^-) and report its
18 dynamics.

19 Phosphorus-doped n-type diamond samples were epitaxially grown by CVD onto Ib-type (111)-
20 oriented diamond substrates with phosphorus concentrations of 5×10^{16} atoms/cm³ (sample A) and
21 about 5×10^{15} atoms/cm³ (sample B) [38]. A homebuilt confocal microscope system was used to
22 optically address single NV centers [38]. All experiments were conducted at room temperature.

23 No color centers other than single NV centers were detected in our high-quality samples under
24 visible illumination. Typically, a high incorporation of nitrogen (such as more than 10^{15} atoms/cm³)
25 during CVD growth generates many NV centers. It makes difficult to detect single NV centers. The

1 fact that we detect many single NV centers in our samples reflects an advantage of phosphorus
2 doping. Figures 1(b) and 1(c) show PL raster scan images of n-type diamond (sample A) illuminated
3 at 532 and 593 nm, respectively. Upon 532 nm illumination, the single NV center, labeled NV1,
4 produces almost the same count rate (~ 55 kcounts/s) as does the NV center labeled NV2. Upon 593
5 nm illumination, the counts rates of NV1 decreases because of the reduced NV^- population, as
6 reported previously [17]. However, the counts rates from NV2 is about five times larger than that
7 from NV1 (50 vs 10 kcounts/s). Moreover, in another area of samples A and B, more than ten single
8 NV centers are bright under 593 nm illumination.

9 Weak excitation (typically $1 \mu W$) at 593 nm wavelength makes the charge-state interconversion
10 of NV center gently. Thereby this is used to real-time detection of the charge states [17]. The charge
11 states are distinguished by photon counts with optical filters (we used a 650-nm longpass filter)
12 which blocks the fluorescence of NV^0 . From the real-time fluorescence trace of NV1, shown in Fig.
13 2(a), the optically induced charge-state interconversion is recorded as telegraph signals of
14 fluorescence from NV^- (high counts) and NV^0 (low counts). In contrast to NV1, NV2 continuously
15 keeps the fluorescence level of NV^- (Fig. 2(b)). These results suggest that NV2 populates to pure
16 NV^- under $1 \mu W$, 593 nm illumination.

17 In order to know charge-state population under 532 nm and 593 nm illumination, photon
18 statistic measurements after illumination are performed. At NV1, average lifetimes of NV^0 and NV^-
19 are 2.92 and 0.59 s, respectively, as determined by the hidden Markov model [17]. Therefore, for
20 detection with $1 \mu W$ illumination at 593 nm, if the detection time is sufficiently less than 0.59 s, we
21 can nondestructively determine charge-states population from histogram of photon counts after
22 arbitrarily initialization (single-shot charge-state measurement). Figures 3(a) and 3(b) are
23 measurement sequences and histograms of photon counts of NV1 after initialization by $30 \mu W$, 532
24 nm and $1 \mu W$, 593 nm illumination. For both initializations, the charge-state population of NV1 has
25 a double Poisson distribution. For initialization at 532 nm, the charge-state populations are estimated

1 to be $NV^0 : NV^- = 0.21 : 0.79$ from area of each peaks. Upon initialization at 593 nm, NV^- decreases
2 to 0.12 on NV1 (Fig. 3(b)). These populations are almost the same as single NV centers in intrinsic
3 diamond [17]. In contrast to NV1, NV2 has only one peak on the both sequences (Figs. 3(c) and
4 3(d)). Peak widths and positions are quite similar to those of NV^- in Fig. 3(a). This result strongly
5 suggests that detected photons in single-shot measurements come from pure NV^- . The difference in
6 the NV^- population between NV1 and NV2 might be attributed to their different local environments
7 (i.e., impurity and/or defects).

8 On the other hand, under 100 μW , 532 nm illumination, the PL spectrum and the optically
9 detected magnetic resonance (ODMR) intensity of NV^- on NV2 are the same as those of NV1 [38].
10 These results suggest that, under 100 μW , 532 nm illumination, the charge-state population of NV2
11 is the same as that of NV1, despite a single peak being observed in Fig. 3(c). This fact implies that
12 the charge state changes during the dark period (10 ms) between initialization and detection. To
13 elucidate this fact, we average the PL intensity of NV2 after a time delay T_d . A 593 nm illumination
14 with power of 230 μW is used to observe decay of fluorescence. The measurement sequence and
15 results are shown in Fig. 4(a). For $T_d = 0.1$ ms, the PL intensity does not change during illumination.
16 This means the charge state of NV2 is in a state of equilibrium during T_d and illumination. However,
17 when T_d increases to 50 ms, increases of intensity and exponential decay of PL are observed. The
18 increase of intensity can be attributed to the increase of the NV^- population during the dark period
19 (T_d). The subsequent decay is attributed to the decrease of the NV^- population during illumination by
20 relatively higher power (230 μW) compared with 1 μW in single-shot charge-state measurement.

21 To reveal the transition rate of the charge states during T_d , the PL intensity was measured as a
22 function of T_d as shown in Fig. 4(b). The PL intensity clearly increases with T_d up to a saturation
23 level. By fitting with a single exponential function, the transition rate from NV^0 to NV^- during T_d
24 (λ_{dark}^0) is estimated to $1/(3.55 \pm 0.42 \text{ ms}) = 0.282 \pm 0.033 \text{ ms}^{-1}$.

1 Next we investigate the dynamics during 593 nm illumination with several powers to show that
2 the time constant for the charge-state transition is much longer than 30 ms under 1 μW , which is the
3 power of the charge detection in Figure 3. Figures 4(c) and 4(d) show the accumulated PL intensity
4 of NV² under 100 and 1 μW , 593 nm illumination after initialization by 532 nm laser. The time
5 delay T_d between the 532 and 593 nm laser pulses was set to 10 ms, which is long enough for the
6 NV⁻ population to grow to more than 99%. At 100 μW , 593 nm illumination, the PL intensity decays
7 exponentially, as shown in Fig. 4(c). This result indicates that the rate from NV⁻ to NV⁰ by 593 nm
8 illumination ($\lambda_{593\text{nm}}^{0-}$) at 100 μW is greater than $\lambda_{\text{dark}}^{0-} + \lambda_{593\text{nm}}^{0-}$, where $\lambda_{593\text{nm}}^{0-}$ is a rate from NV⁰ to
9 NV⁻ by 593 nm illumination. It was observed that the rate $\lambda_{\text{dark}}^{0-} + \lambda_{593\text{nm}}^{0-}$ becomes smaller as the
10 laser power decreases. At 1 μW illumination, no decay in fluorescence intensity is observed, as
11 shown in Fig. 4(d). This also supports charge-state is at equilibrium and purely populated to NV⁻
12 under 1 μW , 593 nm illumination.

13 We quantitatively estimate population of NV⁻ to use transition rates. Under 593 nm cw
14 illumination, the steady-state-population of NV⁻ (p_{NV^-}) can be calculated as follows [17,34]:

$$15 \quad p_{\text{NV}^-} = \frac{\lambda^{0-}}{\lambda^{0-} + \lambda^{0}} = \frac{\lambda_{593\text{nm}}^{0-} + \lambda_{\text{dark}}^{0-}}{\lambda_{593\text{nm}}^{0-} + \lambda_{\text{dark}}^{0-} + \lambda_{593\text{nm}}^{0}}. \quad (1)$$

16 We omitted $\lambda_{\text{dark}}^{0-}$ because it is negligibly smaller than other rates (if it is not zero, histogram of Figs.
17 2(c) and (d) must contain two Poisson distributions.). Here the optically induced transition rates
18 ($\lambda_{593\text{nm}}^{0-}$ and $\lambda_{593\text{nm}}^0$) for NV1 under 1 μW , 593 nm illumination can be obtained by average lifetimes
19 of NV⁰ and NV⁻ in Fig. 2(a). These rates are estimated to be $\lambda_{593\text{nm}}^{0-} = 1/2.92\text{s} = 0.342\text{s}^{-1}$ and
20 $\lambda_{593\text{nm}}^0 = 1/0.59\text{s} = 1.7\text{s}^{-1}$. If these values of NV2 are assumed to be the same as those for NV1,
21 p_{NV^-} for NV2 under 1 μW , 593 nm illumination is estimated to be $p_{\text{NV}^-} = 0.994 \pm 0.001$ from

1 equation (1). For reference, p_{NV^-} for NV1 is calculated to be 0.170 (where $\lambda_{\text{dark}}^{0-} = 0$), which is
2 consistent with the charge-state population in Fig. 3(b). The case for the 532 nm excitation can be
3 analyzed and it is indicated that a population consisting solely of the NV^- charge state can be
4 generated by low-power 532 nm illumination [38].

5 In NV2, we found a four-fold enhancement of an ODMR under 593 nm excitation compared
6 with that of NV1. Figure 4(e) shows ODMR spectra of NV1 and NV2 with a 1 mT magnetic field
7 along the [111] direction of the diamond crystal under 200 μW , 593 nm illumination. From NV2, the
8 ODMR signal intensity from NV^- , which is the normalized fluorescence intensity, is almost 4.18
9 times larger than that from NV1. This result confirms that the NV^- population of NV2 is much larger
10 than that of NV1 and single peaks in Figs. 3(c) and 3(d) are from the NV^- charge state. To measure
11 the ODMR spectra, we increased the 593 nm laser power to 200 μW . At 200 μW , the charge state is
12 not considered to be a purely negative state. Under 593 nm, 1 μW illumination, the ratio of NV^-
13 population between NV2 and NV1 is calculated to be $100\% / 12\% = 8.33$ from the results of Fig. 3
14 (b) and 3 (d). The enhanced ratio of ODMR signal intensity (= 4.18) is smaller than it. The main
15 reason is considered to be due to the smaller ratio of NV^- population at the high laser power (200
16 μW). In our case, NV1 and NV2 are aligned to [111] direction of diamond crystal. Therefore, we
17 assume the microwave power, the amplitude and the polarization of laser of NV2 are the same with
18 those of NV1. In the general case that NVs feels different microwave power, amplitude and
19 polarization of laser with each other, we need to consider the effects of broadening of the
20 spectra [39].

21 Finally, we measured spin-coherence time T_2 by Hahn echo technique, because a long T_2 is
22 critical for quantum information and sensing. As a result, T_2 is estimated to be $19.77 \pm 0.27 \mu\text{s}$ for
23 NV2 in sample A ($[\text{P}] = 5 \times 10^{16} \text{ atoms/cm}^3$) and $49.6 \pm 2.2 \mu\text{s}$ for sample B ($[\text{P}] = 5 \times 10^{15}$
24 atoms/cm^3) [38]. Previously, dependence of nitrogen donors (i.e., P1 centers) concentration on T_2 of
25 P1 centers was investigated and T_2 of P1 centers is estimated to be about 1 ms and 100 μs for the P1

1 concentration of 5×10^{15} and $5 \times 10^{16} \text{ cm}^{-3}$, respectively [40]. We expect that the dependence of the
2 phosphorus concentration on T_2 of NV centers to be almost the same as that of the P1 center because
3 the unpaired electrons localize on their atoms. However, the present results of T_2 are shorter than the
4 expected values. It can be attributed to other impurities or defects [41]. In other words, if these
5 impurities or defects could be removed and if ^{12}C could be enriched, T_2 in n-type diamond should
6 become comparable to the long (millisecond order) T_2 of high-quality intrinsic ^{12}C -enriched
7 diamond [13,42].

8 In summary, we investigated the NV^- population and its dynamics in phosphorus-doped n-type
9 diamond by using nondestructive, single-shot readout measurements of the NV charge state. In
10 phosphorus-doped n-type diamond, the results reveal that the NV^- charge state that populates over
11 99% of the NV centers is generated by $1 \mu\text{W}$ illumination at 593 nm. Under these illumination
12 conditions, we obtain an almost five-fold increase in luminescence and a four-fold increase in the
13 ODMR signal compared with the corresponding results for NV centers in intrinsic diamond. By
14 analyzing the NV^- population as a function of illumination, we show that this approach would
15 increase the NV^- population not only under 593 nm illumination but also under illumination by other
16 wavelengths, such as 532 nm. These results are expected to significantly enhance the versatile
17 potential of NV centers.

18
19 This work was supported by JSPS KAKENHI Grant Number 15J05801. The authors gratefully
20 acknowledge the financial support from NICT, as well as from JST CREST program. FJ
21 acknowledges DFG, EU, ERC, Volkswagenstiftung, and DARPA.

22
23
24

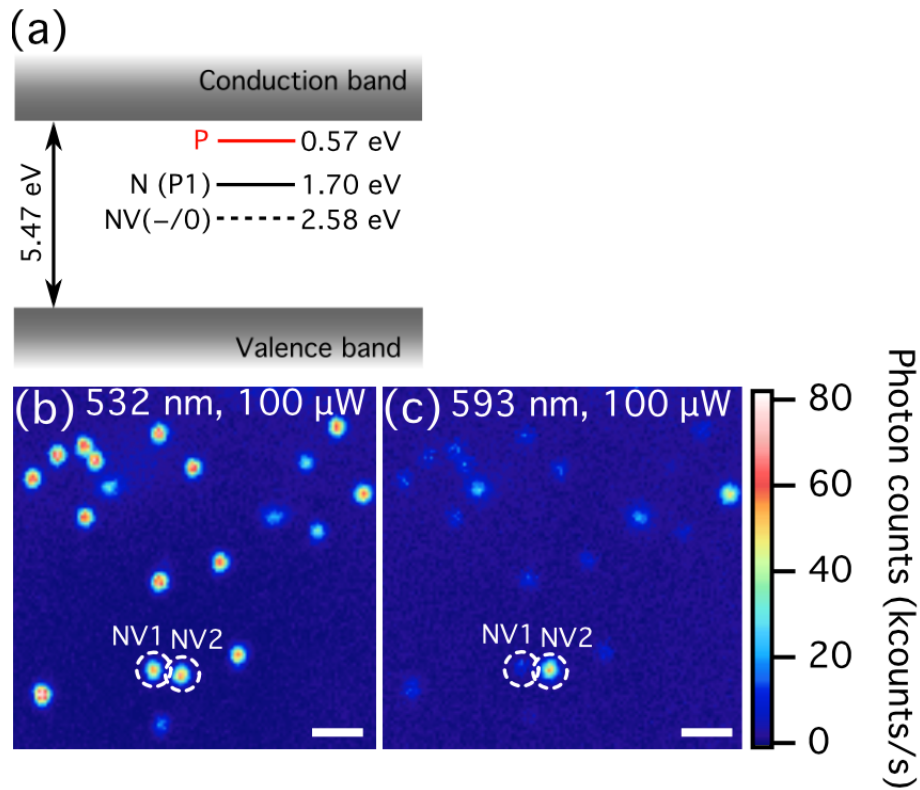
1 REFERENCES

- 2 [1] G. Waldherr, Y. Wang, S. Zaiser, M. Jamali, T. Schulte-Herbrüggen, H. Abe, T.
3 Ohshima, J. Isoya, J. F. Du, P. Neumann, and J. Wrachtrup, *Nature (London)* **506**, 204
4 (2014).
- 5 [2] P. C. Maurer, G. Kucsko, C. Latta, L. Jiang, N. Y. Yao, S. D. Bennett, F. Pastawski, D.
6 Hunger, N. Chisholm, M. Markham, D. J. Twitchen, J. I. Cirac, and M. D. Lukin, *Room-*
7 *temperature quantum bit memory exceeding one second.*, *Science* **336**, 1283 (2012).
- 8 [3] T. van der Sar, Z. H. Wang, M. S. Blok, H. Bernien, T. H. Taminiau, D. M. Toyli, D. A.
9 Lidar, D. D. Awschalom, R. Hanson, and V. V. Dobrovitski, *Nature (London)* **484**, 82
10 (2012).
- 11 [4] H. Bernien, B. Hensen, W. Pfaff, G. Koolstra, M. S. Blok, L. Robledo, T. H. Taminiau,
12 M. Markham, D. J. Twitchen, L. Childress, and R. Hanson, *Nature (London)* **497**, 86
13 (2013).
- 14 [5] L. Robledo, L. Childress, H. Bernien, B. Hensen, P. F. A. Alkemade, and R. Hanson,
15 *Nature (London)* **477**, 574 (2011).
- 16 [6] P. Neumann, J. Beck, M. Steiner, F. Rempp, H. Fedder, P. R. Hemmer, J. Wrachtrup,
17 and F. Jelezko, *Single-shot readout of a single nuclear spin*, *Science* **329**, 542 (2010).
- 18 [7] L. Childress, M. V. G. Dutt, J. M. Taylor, A. S. Zibrov, F. Jelezko, J. Wrachtrup, P. R.
19 Hemmer, and M. D. Lukin, *Coherent dynamics of coupled electron and nuclear spin*
20 *qubits in diamond.*, *Science* **314**, 281 (2006).
- 21 [8] V. Jacques, E. Wu, F. Grosshans, F. Treussart, P. Grangier, A. Aspect, and J.-F.
22 Roch, *Experimental Realization of Wheeler's Delayed-Choice Gedanken Experiment*,
23 *Science* **315**, 966 (2007).
- 24 [9] J. R. Maze, P. L. Stanwix, J. S. Hodges, S. Hong, J. M. Taylor, P. Cappellaro, L. Jiang,
25 M. V. G. Dutt, E. Togan, A. S. Zibrov, A. Yacoby, R. L. Walsworth, and M. D. Lukin,
26 *Nanoscale magnetic sensing with an individual electronic spin in diamond*, *Nature*
27 *(London)* **455**, 644 (2008).
- 28 [10] G. Balasubramanian, I. Y. Chan, R. Kolesov, M. Al-Hmoud, J. Tisler, C. Shin, C. Kim,
29 A. Wojcik, P. R. Hemmer, A. Krueger, T. Hanke, A. Leitenstorfer, R. Bratschitsch, F.
30 Jelezko, and J. Wrachtrup, *Nature (London)* **455**, 648 (2008).
- 31 [11] H. J. Mamin, M. Kim, M. H. Sherwood, C. T. Rettner, K. Ohno, D. D. Awschalom, and
32 D. Rugar, *Nanoscale Nuclear Magnetic Resonance with a Nitrogen-Vacancy Spin*
33 *Sensor*, *Science* **339**, 557 (2013).
- 34 [12] F. Shi, X. Kong, P. Wang, F. Kong, N. Zhao, R.-B. Liu, and J. Du, *Sensing and atomic-*
35 *scale structure analysis of single nuclear-spin clusters in diamond*, *Nat. Phys.* **10**, 21
36 (2013).
- 37 [13] G. Balasubramanian, P. Neumann, D. J. Twitchen, M. Markham, R. Kolesov, N.
38 Mizuochi, J. Isoya, J. Achard, J. Beck, J. Tisler, V. Jacques, P. R. Hemmer, F.
39 Jelezko, and J. Wrachtrup, *Ultralong spin coherence time in isotopically engineered*
40 *diamond.*, *Nat. Mater.* **8**, 383 (2009).
- 41 [14] L. P. McGuinness, Y. Yan, A. Stacey, D. A. Simpson, L. T. Hall, D. Maclaurin, S.
42 Praver, P. Mulvaney, J. Wrachtrup, F. Caruso, R. E. Scholten, and L. C. L. Hollenberg,
43 *Quantum measurement and orientation tracking of fluorescent nanodiamonds inside*
44 *living cells*, *Nat. Nanotechnol.* **6**, 358 (2011).
- 45 [15] T. Staudacher, F. Shi, S. Pezzagna, J. Meijer, J. Du, C. A. Meriles, F. Reinhard, and J.
46 Wrachtrup, *Nuclear Magnetic Resonance Spectroscopy on a (5-Nanometer)³ Sample*
47 *Volume*, *Science* **339**, 561 (2013).
- 48 [16] D. Le Sage, K. Arai, D. R. Glenn, S. J. DeVience, L. M. Pham, L. Rahn-Lee, M. D.
49 Lukin, A. Yacoby, A. Komeili, and R. L. Walsworth, *Nature* **496**, 486 (2013).

- 1 [17] N. Aslam, G. Waldherr, P. Neumann, F. Jelezko, and J. Wrachtrup, *Photo-induced*
2 *ionization dynamics of the nitrogen vacancy defect in diamond investigated by single-*
3 *shot charge state detection*, New J. Phys. **15**, 013064 (2013).
- 4 [18] P. Siyushev, H. Pinto, M. Vörös, A. Gali, F. Jelezko, and J. Wrachtrup, *Optically*
5 *Controlled Switching of the Charge State of a Single Nitrogen-Vacancy Center in*
6 *Diamond at Cryogenic Temperatures*, Phys. Rev. Lett. **110**, 167402 (2013).
- 7 [19] A. S. Trifonov, J. C. Jaskula, C. Teulon, D. R. Glenn, N. Bar-Gill, and R. L. Walsworth,
8 *Limits to Resolution of CW STED Microscopy*, Adv. At., Mol., Opt. Phys. **62**, 279
9 (2013).
- 10 [20] X.-D. Chen, C.-L. Zou, F.-W. Sun, and G.-C. Guo, *Optical manipulation of the charge*
11 *state of nitrogen-vacancy center in diamond*, Appl. Phys. Lett. **103**, 013112 (2013).
- 12 [21] G. Waldherr, J. Beck, M. Steiner, P. Neumann, A. Gali, T. Frauenheim, F. Jelezko, and
13 J. Wrachtrup, *Dark states of single nitrogen-vacancy centers in diamond unraveled by*
14 *single shot NMR.*, Phys. Rev. Lett. **106**, 157601 (2011).
- 15 [22] A. Stacey, D. A. Simpson, T. J. Karle, B. C. Gibson, V. M. Acosta, Z. Huang, K.-M. C.
16 Fu, C. Santori, R. G. Beausoleil, L. P. McGuinness, K. Ganesan, S. Tomljenovic-
17 Hanic, A. D. Greentree, and S. Prawer, *Near-surface spectrally stable nitrogen*
18 *vacancy centres engineered in single crystal diamond.*, Adv. Mater. **24**, 3333 (2012).
- 19 [23] V. M. Acosta, C. Santori, A. Faraon, Z. Huang, K.-M. C. Fu, A. Stacey, D. A. Simpson,
20 K. Ganesan, S. Tomljenovic-Hanic, A. D. Greentree, S. Prawer, and R. G. Beausoleil,
21 *Dynamic Stabilization of the Optical Resonances of Single Nitrogen-Vacancy Centers*
22 *in Diamond*, Phys. Rev. Lett. **108**, 206401 (2012).
- 23 [24] B. K. Ofori-Okai, S. Pezzagna, K. Chang, M. Loretz, R. Schirhagl, Y. Tao, B. A.
24 Moores, K. Groot-Berning, J. Meijer, and C. L. Degen, *Spin properties of very shallow*
25 *nitrogen vacancy defects in diamond*, Phys. Rev. B **86**, 081406 (2012).
- 26 [25] K. Y. Y. Han, S. K. Kim, C. Eggeling, and S. W. Hell, *Metastable dark States enable*
27 *ground state depletion microscopy of nitrogen vacancy centers in diamond with*
28 *diffraction-unlimited resolution.*, Nano Lett. **10**, 3199 (2010).
- 29 [26] Y. Mita, *Change of absorption spectra in type-Ib diamond with heavy neutron*
30 *irradiation.*, Phys. Rev. B **53**, 11360 (1996).
- 31 [27] C. Bradac, T. Gaebel, N. Naidoo, M. J. Sellars, J. Twamley, L. J. Brown, A. S. Barnard,
32 T. Plakhotnik, A. V. Zvyagin, and J. R. Rabeau, *Observation and control of blinking*
33 *nitrogen-vacancy centres in discrete nanodiamonds.*, Nat. Nanotechnol. **5**, 345 (2010).
- 34 [28] M. V. Hauf, B. Grotz, B. Naydenov, M. Dankerl, S. Pezzagna, J. Meijer, F. Jelezko, J.
35 Wrachtrup, M. Stutzmann, F. Reinhard, and J. A. Garrido, *Chemical control of the*
36 *charge state of nitrogen-vacancy centers in diamond*, Phys. Rev. B **83**, 081304 (2011).
- 37 [29] T. W. Shanley, A. A. Martin, I. Aharonovich, and M. Toth, *Localized chemical switching*
38 *of the charge state of nitrogen-vacancy luminescence centers in diamond*, Appl. Phys.
39 Lett. **105**, 063103 (2014).
- 40 [30] N. Mizuochi, T. Makino, H. Kato, D. Takeuchi, M. Ogura, H. Okushi, M. Nothaft, P.
41 Neumann, A. Gali, F. Jelezko, J. Wrachtrup, and S. Yamasaki, *Electrically driven*
42 *single-photon source at room temperature in diamond*, Nat. Photonics **6**, 299 (2012).
- 43 [31] B. Grotz, M. V. Hauf, M. Dankerl, B. Naydenov, S. Pezzagna, J. Meijer, F. Jelezko, J.
44 Wrachtrup, M. Stutzmann, F. Reinhard, and J. A. Garrido, *Charge state manipulation*
45 *of qubits in diamond.*, Nat. Commun. **3**, 729 (2012).
- 46 [32] H. Kato, M. Wolfer, C. Schreyvogel, M. Kunzer, W. Müller-Sebert, H. Obloh, S.
47 Yamasaki, and C. E. Nebel, *Tunable light emission from nitrogen-vacancy centers in*
48 *single crystal diamond PIN diodes*, Appl. Phys. Lett. **102**, 151101 (2013).
- 49 [33] M. V. Hauf, P. Simon, N. Aslam, M. Pfender, P. Neumann, S. Pezzagna, J. Meijer, J.
50 Wrachtrup, M. Stutzmann, F. Reinhard, and J. A. Garrido, *Addressing single nitrogen-*

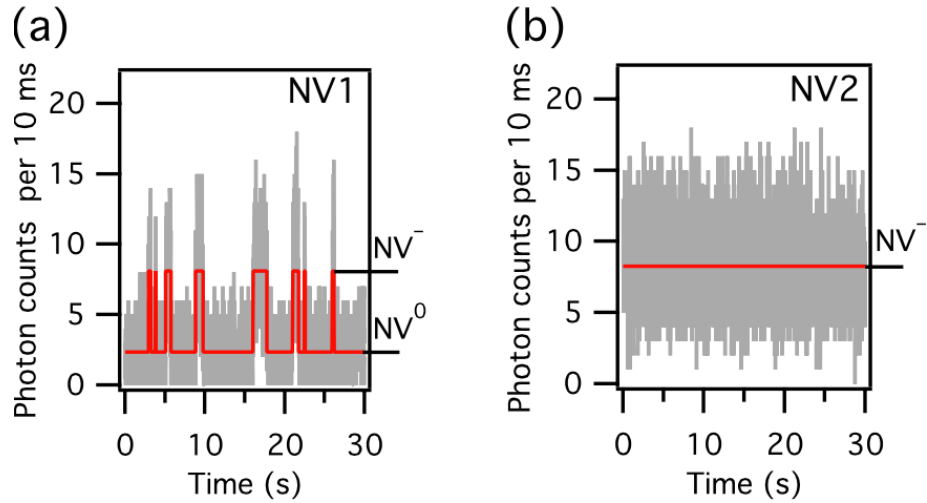
- 1 *vacancy centers in diamond with transparent in-plane gate structures.*, Nano Lett. **14**,
2 2359 (2014).
- 3 [34] Y. Doi, T. Makino, H. Kato, D. Takeuchi, M. Ogura, H. Okushi, H. Morishita, T.
4 Tashima, S. Miwa, S. Yamasaki, P. Neumann, J. Wrachtrup, Y. Suzuki, and N.
5 Mizuochi, *Deterministic Electrical Charge-State Initialization of Single Nitrogen-*
6 *Vacancy Center in Diamond*, Phys. Rev. X **4**, 011057 (2014).
- 7 [35] J. P. Goss, P. R. Briddon, R. Jones, and S. Sque, *Donor and acceptor states in*
8 *diamond*, Diam. Relat. Mater. **13**, 684 (2004).
- 9 [36] K. Groot-Berning, N. Raatz, I. Dobrinets, M. Lesik, P. Spinicelli, A. Tallaire, J. Achard,
10 V. Jacques, J.-F. Roch, A. M. Zaitsev, J. Meijer, and S. Pezzagna, *Passive charge*
11 *state control of nitrogen-vacancy centres in diamond using phosphorous and boron*
12 *doping*, Phys. Status Solidi A **211**, 2268 (2014).
- 13 [37] M. Katagiri, J. Isoya, S. Koizumi, and H. Kanda, *Lightly phosphorus-doped*
14 *homoepitaxial diamond films grown by chemical vapor deposition*, Applied Physics
15 Letters **85**, 6365 (2004).
- 16 [38] See Suplimental Materials at [URL will be inserted by publisher] for details of the
17 experiments.
- 18 [39] A. Dréau, M. Lesik, L. Rondin, P. Spinicelli, O. Arcizet, J.-F. Roch, and V. Jacques,
19 *Avoiding power broadening in optically detected magnetic resonance of single NV*
20 *defects for enhanced dc magnetic field sensitivity*, Physical Review B **84**, 195204
21 (2011).
- 22 [40] J. A. van Wyk, E. C. Reynhardt, G. L. High, and I. Kiflawi, *The dependences of ESR*
23 *line widths and spin-spin relaxation times of single nitrogen defects on the*
24 *concentration of nitrogen defects in diamond*, J. Phys. D: Appl. Phys. **30**, 1790 (1997).
- 25 [41] N. Mizuochi, H. Watanabe, J. Isoya, H. Okushi, and S. Yamasaki, *Hydrogen-related*
26 *defects in single crystalline CVD homoepitaxial diamond film studied by EPR*, Diam.
27 Relat. Mater. **13**, 765 (2004).
- 28 [42] N. Mizuochi, P. Neumann, F. Rempp, J. Beck, V. Jacques, P. Siyushev, K. Nakamura,
29 D. J. Twitchen, H. Watanabe, S. Yamasaki, F. Jelezko, and J. Wrachtrup, *Coherence*
30 *of single spins coupled to a nuclear spin bath of varying density*, Phys. Rev. B **80**,
31 041201 (2009).
- 32
- 33

1
2 **FIGURES**



3
4 Figure 1: (a) Donor energy levels of phosphorus (P) and nitrogen (P1) donors and acceptor level
5 labelled (-/0) of the NV center with respect to conduction-band edge of diamond. (b) PL raster-scan
6 images of single NV centers in n-type diamond (sample A, $[P] = 5 \times 10^{16}$ atoms/cm³) under 100 μW,
7 532 nm illumination. Most single NVs show similar optical properties under these illumination
8 conditions. (c) Same as panel (b) but for 100 μW, 593 nm illumination. Fluorescence count rate of
9 NV2 is about five times larger than that of NV1.
10

1



2

3 Figure 2: (a) Time trace of fluorescence of NV1 under continuous 1 μ W, 593 nm illumination.

4 Photon bursts occur when the charge state transforms into the NV⁻ state. The solid red line shows the

5 most probable fluorescence levels, as obtained by the hidden Markov model. Here the average

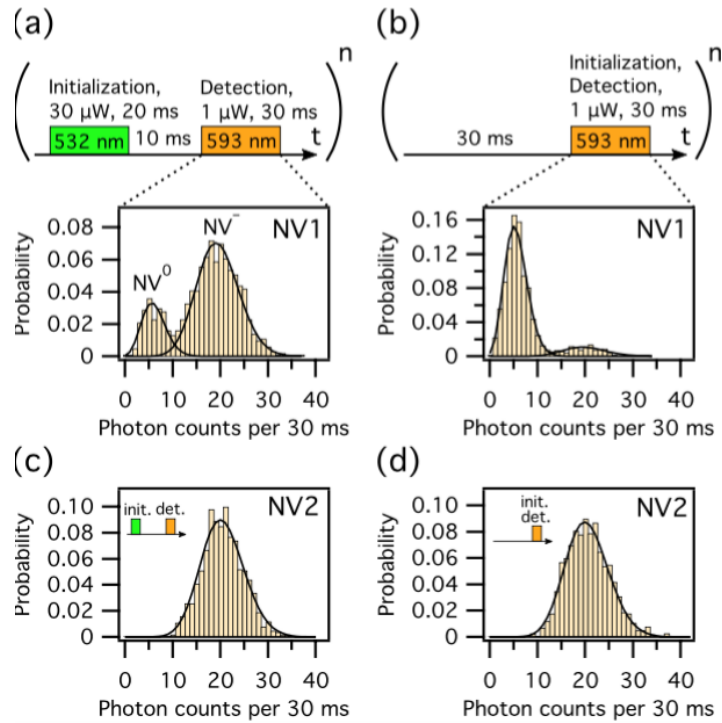
6 lifetimes of the two charge states are 2.92 s (NV⁰) and 0.59 s (NV⁻). (b) Time trace of fluorescence

7 of NV2 under the same illumination condition as for NV1. NV2 does not show photon bursts in the

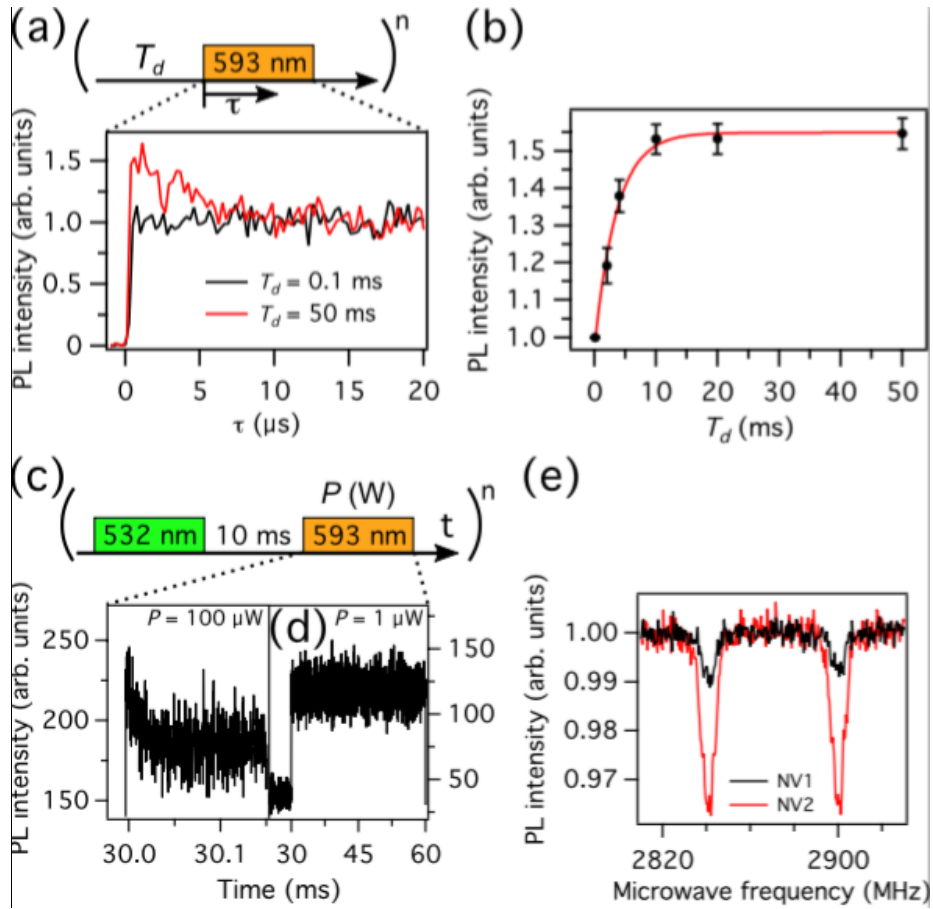
8 trace. A solid red line is the average count rate and is almost the same as the higher counts (NV⁻) of

9 NV1 in panel (a).

10



1
 2 Figure 3: Nondestructive single-shot charge-state measurements with two types of charge state
 3 initialization: (a) 30 μ W, 532 nm illumination and (b) 1 μ W, 593 nm illumination. NV1 population
 4 exhibits a double Poisson distribution that is due to two different charge states. Initialization at 593
 5 nm drastically decreases the population of the NV^- charge state. (c), (d) Conversely, NV2 has a
 6 single peak at the same position as NV^- irrespective of initialization conditions. We repeated each
 7 sequence $n=1000$ times for each histogram.



1
2 Figure 4: (a) Increase of initial PL intensity of NV2 after time delay $T_d = 0.1$ and 50 ms under 230
3 μW , 593 nm illumination. PL intensity of NV2 increases after $T_d = 50$ ms. We repeated sequence
4 $n=12,209$ times. (b) PL intensity as a function of T_d . The fluorescence intensity is normalized to
5 unity for $T_d = 0.1$ ms. The solid red line is a fit to a monoexponential with a time constant of 3.55
6 ms. (c) PL intensity for 593 nm illumination pulse $T_d = 10$ ms after initialization by 532 nm
7 illumination pulse. For 100 μW illumination, the PL intensity decays exponentially. (d) Same
8 measurement as for panel (c) except the illumination was 1 μW , 593 nm. No decay in fluorescence
9 intensity is observed. We repeated sequence $n=17,219$ and 9130 for $P = 100$ μW and 1 μW
10 illumination, respectively. (e) ODMR spectrum of NV1 and NV2 under 200 μW , 593 nm
11 illumination. Signal intensity from NV⁻ of NV2 is almost 4.18 times larger than that from NV1.. The
12 amplitude of the applied magnetic field was 1 mT along the [111] direction of the diamond crystal.